

Unravelling Electron Transfer in Peptide-Cation Complexes: A Model for Mimicking Redox Centres in Proteins

Jingxian Yu,* John R. Horsley, and Andrew D. Abell*

ARC Centre of Excellence for Nanoscale BioPhotonics (CNBP), Institute of Photonics and Advanced Sensing (IPAS), Department of Chemistry, The University of Adelaide, Adelaide, SA 5005, Australia

Table of Contents:

1. Materials	Page S2
2. Peptide synthesis	Page S2
3. ROESY spectra of peptides 1-4	Page S7
4. ¹ H NMR titration study of peptide 3	Page S12
5. Computational models of peptides 1 and 3 (unbound and with zinc)	Page S13
6. Electrochemical data for peptide 4	Page S18
7. Switching data for β -strand peptide 2	Page S19
8. Quantum transport simulations	Page S20
9. Constrained density functional theory (cDFT) calculations	Page S22
10. Mass Spectroscopy	Page S23
11. ¹ H NMR spectra for target peptides	Page S25
12. References	Page S28

1. Materials

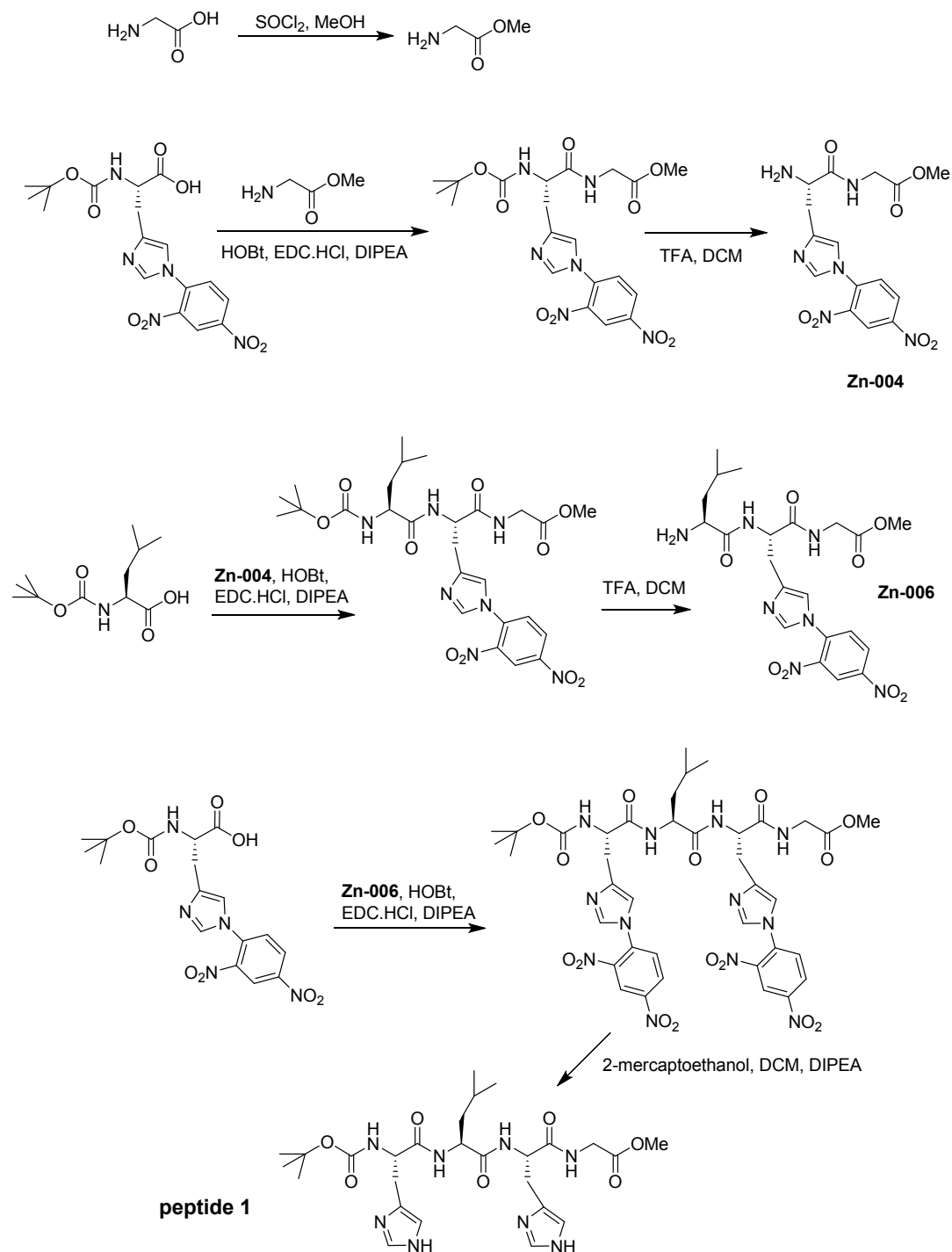
Fmoc-Cys(mmt)-OH, Boc-His(DNP)-OH, diisopropylethylamine (DIPEA), triisopropylsilane (TIPS), trifluoroacetic acid (TFA), and 2-mercaptoethanol were purchased from Sigma-Aldrich, Australia. Boc-Aib-OH, Fmoc-Leu-OH, Fmoc-His(mtt)-OH, and 2-(1H-7-azabenzotriazol-1-yl)-1,1,3,3-tetramethyl uranium hexafluorophosphate methanaminium (HATU) were purchased from Chem Impex, USA. Hydroxybenzotriazole (HOBt), 1-Ethyl-3-(3-dimethylaminopropyl) carbodiimide (EDC·HCl), and Sieber amide resin were purchased from GL Biochem, China. Ferroceneacetic acid was purchased from Tokyo Chemical Industry Co., Japan. *N,N*-dimethylformamide (DMF), dichloromethane (DCM), thionyl chloride (SOCl₂), methanol (MeOH), piperidine and acetonitrile (CH₃CN) were purchased from Merck, Australia. All solvents and reagents were used without purification unless noted.

2. Peptide synthesis

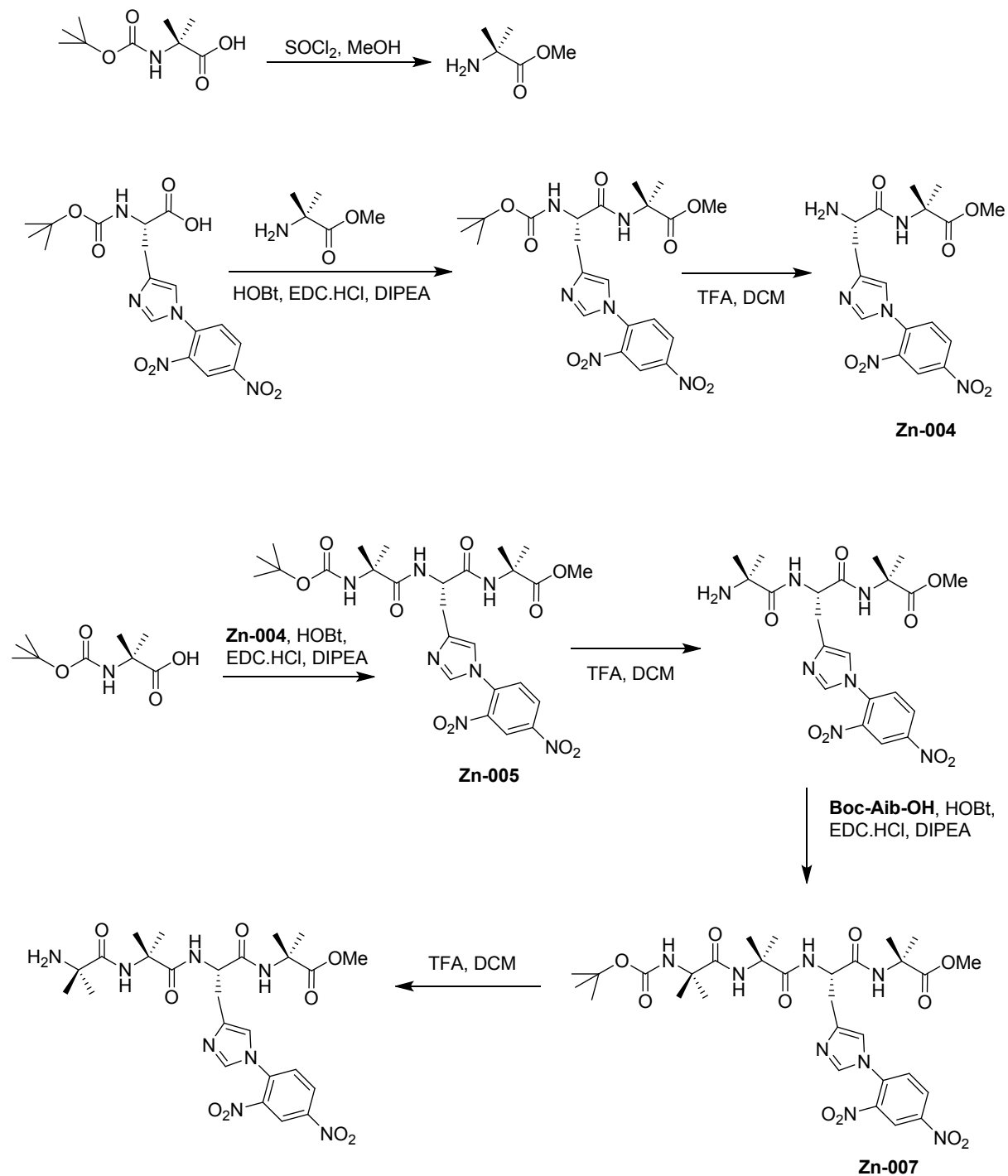
Peptides **1** and **3** were each synthesized using solution phase synthesis, as outlined in Schemes 1 and 2, and purified using reverse phase HPLC. Peptides **2** and **4** were synthesized using Solid Phase Peptide Synthesis (SPPS), with standard Fmoc-based methods and commercially available reagents.

Fmoc-Cys(mmt) was preloaded onto Sieber amide resin with a loading of 0.8 mmol/g resin. The unreacted sites on the resin were capped with acetic acid/pyridine (3:2, 2×25 mL) for 30 min before washing the resin with DCM (×3), DMF (×3) and DCM (×3). *N*-Fmoc deprotection was carried out by treating the resin with 25% piperidine/DMF (25 mL) for 30 min before washing with DCM (×3), DMF (×3) and DCM (×3). Further couplings of amino acids were performed using the following molar ratios of reagents: Fmoc-amino acids (1 equiv.) dissolved in DMF (20 mL), 0.5M HATU/DMF (1 equiv.) and DIPEA (4 equiv.). Fmoc-His(mtt)-OH and ferroceneacetic acid were used for both peptides. The resin was washed with DCM (×3), DMF (×3), DCM (×3) and coupling procedures repeated. The coupling time in all cases was a minimum of 2 h. Deprotection and coupling procedures were repeated alternatively until the sequences were completed. The peptides were then deprotected, the resin washed with DCM (×3), DMF (×3), DCM (×3) and dried under vacuum. The peptides were cleaved from the resin using DCM/TFA/TIPS (90:7.5:2.5, 2×20 mL for 15 min each) and the filtrate collected. The solvent was removed *in vacuo* and the crude products purified using reverse phase HPLC.

Scheme 1. Synthesis of peptide 1.



Scheme 2. Synthesis of peptide 3.



Peptide 1. ¹H NMR (500 MHz, DMSO-d₆) δ 8.96 (s, 2H, imidazole 2×Nε¹), 8.39-8.36 (m, 2H, NH His, NH Gly), 7.96 (d, 1H, NH Leu, *J* = 7.5 Hz), 7.34 (s, 1H, imidazole Nδ²), 7.31 (s, 1H, imidazole Nδ²), 7.09 (d, 1H, NH His, *J* = 9.0 Hz), 4.63-4.59 (m, 1H, CαH, His), 4.30-4.25 (m, 2H, 2×CαH, His, Leu), 3.93-3.82 (ddd, 2H, CH₂ Gly, *J* = 40.6, 17.4, 5.9 Hz), 3.62 (s, 3H, OCH₃), 3.13-2.84 (m, 4H, 2×CH₂), 1.60-1.54 (m, 1H, CH), 1.49-1.39 (m, 2H, CH₂), 1.33 (s, 9H, Boc, 3×CH₃), 0.87-0.82 (m, 6H, 2×CH₃, Leu). HRMS [M]⁺ calc'd = 577.3098, [M]⁺ found = 577.2960.

Peptide 2. ¹H NMR (600 MHz, DMSO-d₆) δ 8.92 (s, 2H, imidazole 2×Nε¹), δ 8.46 (d, 1H, NH His, *J* = 7.8 Hz), 8.17 (d, 1H, NH His, *J* = 8.7 Hz), 8.11 (d, 1H, NH Leu, *J* = 7.5 Hz), δ 7.99 (d, 1H, NH Cys, *J* = 7.7 Hz), 7.56 (s, 1H, terminal NHH), 7.36 (s, 1H, imidazole Nδ²), 7.32 (s, 1H, terminal NHH), 7.27 (s, 1H, imidazole Nδ²), 4.61- 4.58 (m, 2H, 2×CαH, 2×His), 4.34-4.30 (m, 1H, CαH, Cys), 4.26-4.23 (m, 1H, CαH, Leu), 4.13-4.07 (m, 9H, Cp), 4.04 (m, 2H, CH₂), 3.10-2.73 (m, 6H, 3×CH₂), 1.55-1.52 (m, 1H, CH), 1.46-1.41 (m, 2H, CH₂), 0.85-0.80 (m, 6H, Leu 2×CH₃). HRMS [M+H]⁺ calc'd = 734.2536, [M+H]⁺ found = 734.2549.

Peptide 3. ¹H NMR (600 MHz, DMSO-d₆) δ 8.93-8.90 (m, 2H, imidazole 2×Nε¹), 8.61 (d, 1H, NH His, *J* = 4.7 Hz), 8.09 (s, 1H, NH Aib₂), 7.73 (s, 1H, NH Aib₄), 7.56 (d, 1H, NH His, *J* = 8.4 Hz), 7.48 (s, 1H, NH Aib₃), 7.45 (s, 1H, NH Aib₁), 7.34 (s, 2H, imidazole 2×Nδ²), 4.47-4.44 (m, 1H, CαH, His), 4.19-4.15 (m, 1H, CαH, His), 3.52 (s, 3H, OCH₃) 3.25-2.91 (m, 4H, 2×CH₂), 1.39 (s, 9H, Boc, 3×CH₃), 1.35- 1.20 (m, 24H, 8×CH₃, 4×Aib). HRMS [M+Na]⁺ calc'd = 769.3973, [M+Na]⁺ found = 769.3982.

Peptide 4. ¹H NMR (600 MHz, DMSO-d₆) δ 8.97 (s, 2H, imidazole 2×Nε¹), 8.63 (m, 1H, NH Aib₁), 8.40 (m, 1H, NH His), 8.06 (s, 1H, NH Aib₂), 7.83 (s, 1H, NH Aib₃), 7.69 (s, 1H, NH Aib₄), 7.65 (m, 1H, NH His), 7.56 (s, 1H, imidazole Nδ²), 7.40 (m, 1H, NH Cys), 7.37 (s, 1H, imidazole Nδ²), 7.20 (s, 1H, terminal NHH), 7.09 (s, 1H, terminal NHH), 4.40-4.36 (m, 1H, CαH, His), 4.31-4.29 (m, 1H, CαH, His), 4.22-4.21 (m, 1H, CαH, Cys), 4.19-4.12 (m, 9H, Cp), 4.09 (m, 2H, CH₂), 3.29-2.75 (m, 6H, 3×CH₂), 1.41-1.21 (m, 24H, 4×Aib, 8×CH₃). HRMS [M+H]⁺ calc'd = 961.3805, [M+H]⁺ found = 961.3813.

3. ROESY spectra of peptides 1-4.

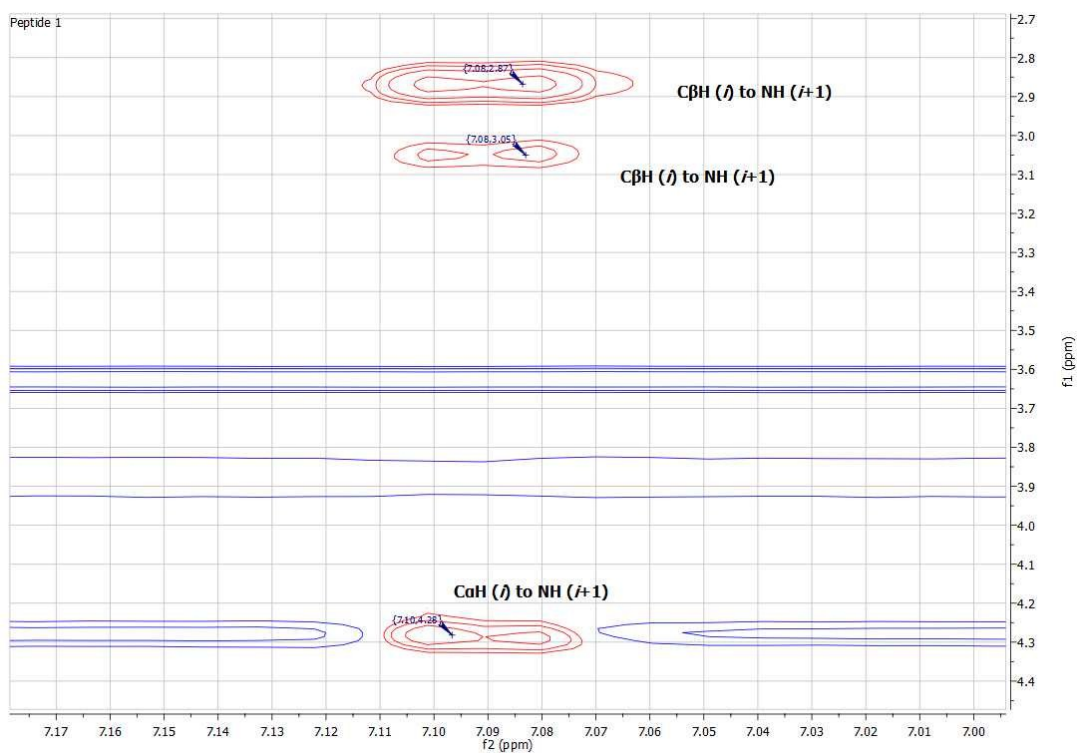


Figure S1. ROESY spectrum of peptide 1 showing $CaH (i)$ to $NH (i+1)$ and $C\beta H_2 (i)$ to $NH (i+1)$ interactions.

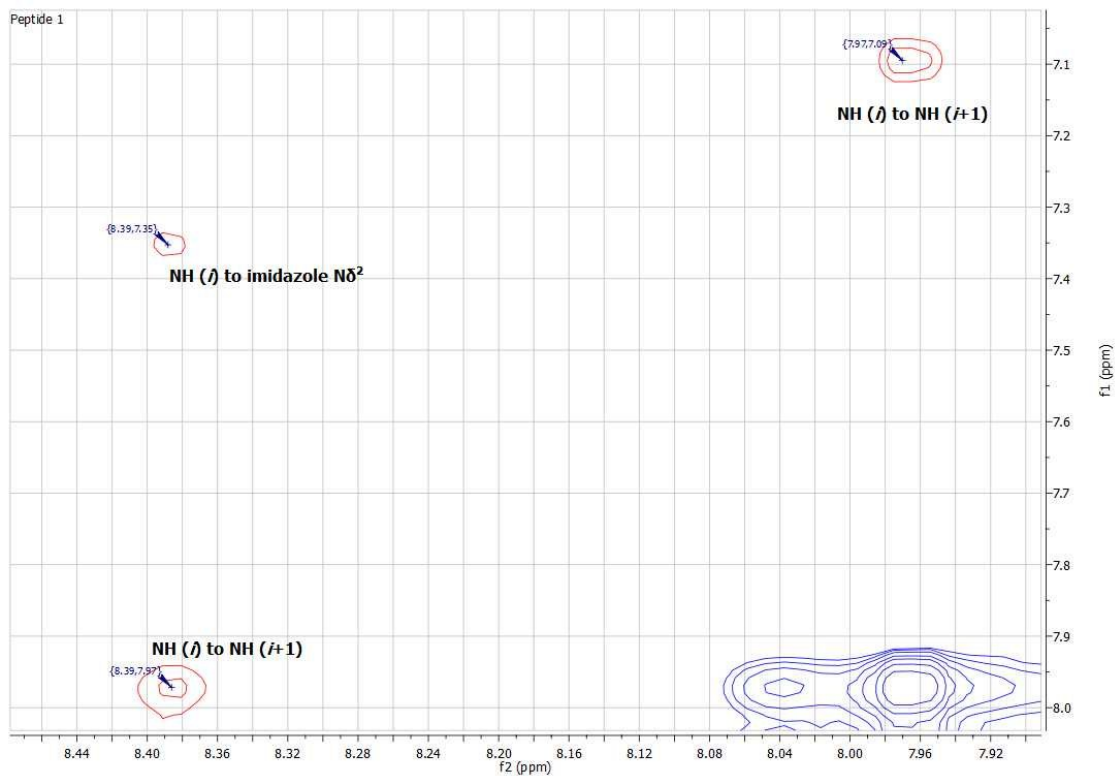


Figure S2. ROESY spectrum of peptide 1 showing $NH (i)$ to $NH (i+1)$ correlations.

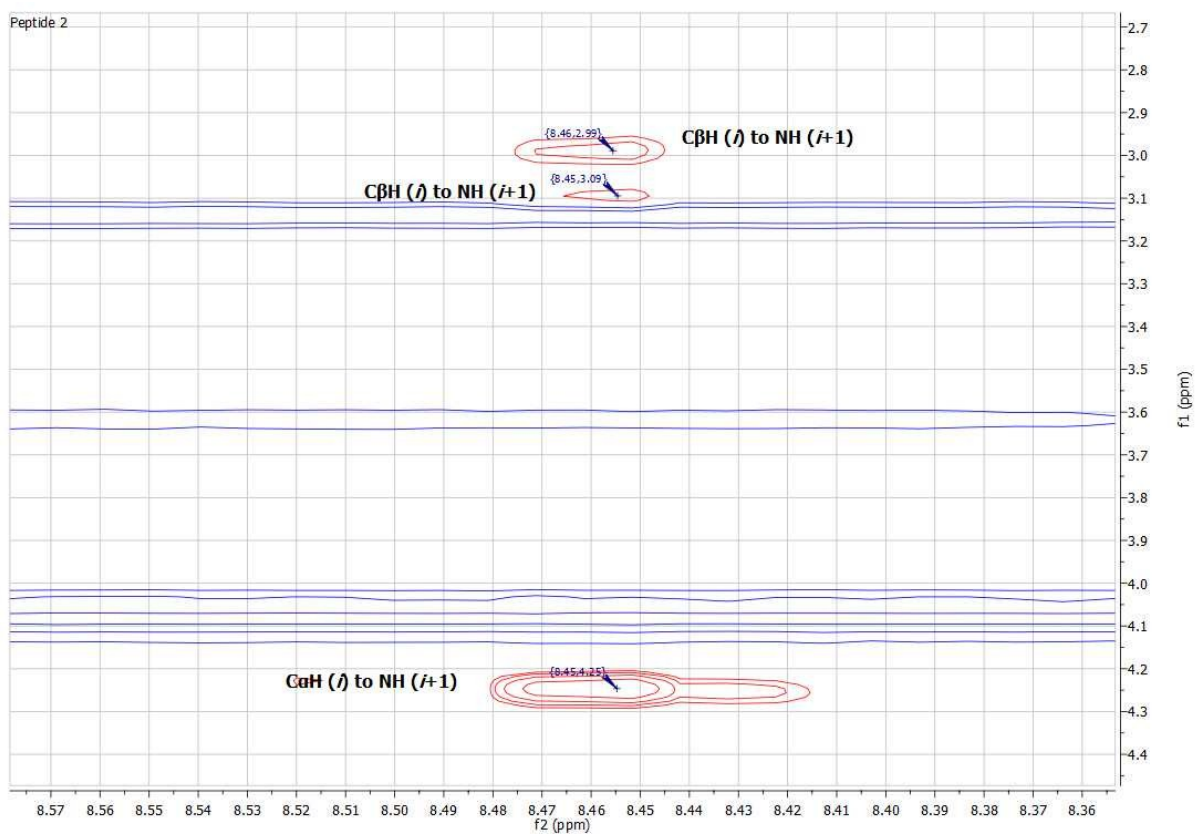


Figure S3. ROESY spectrum of peptide **2** showing CaH (*i*) to NH (*i*+1) and CβH₂ (*i*) to NH (*i*+1) interactions.

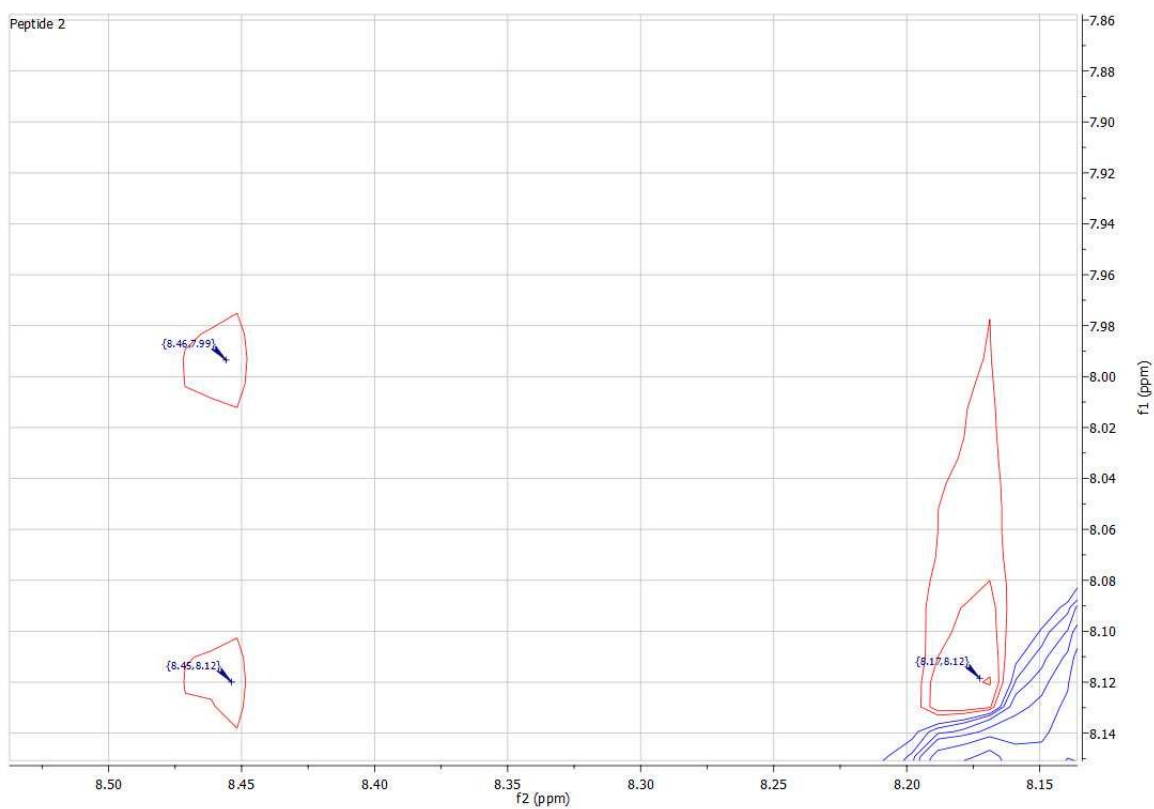


Figure S4. ROESY spectrum of peptide **2** showing NH (*i*) to NH (*i*+1) correlations.

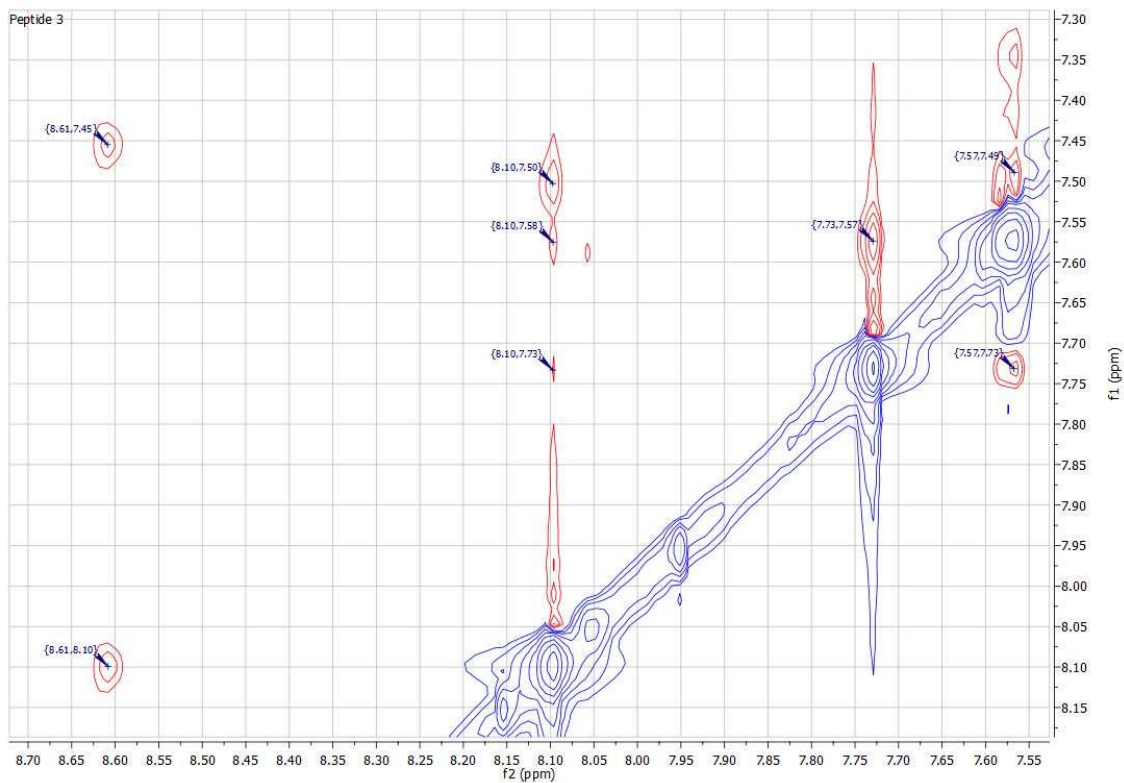


Figure S5. ROESY spectrum of peptide **3** showing NH (*i*) to NH (*i*+1) correlations.

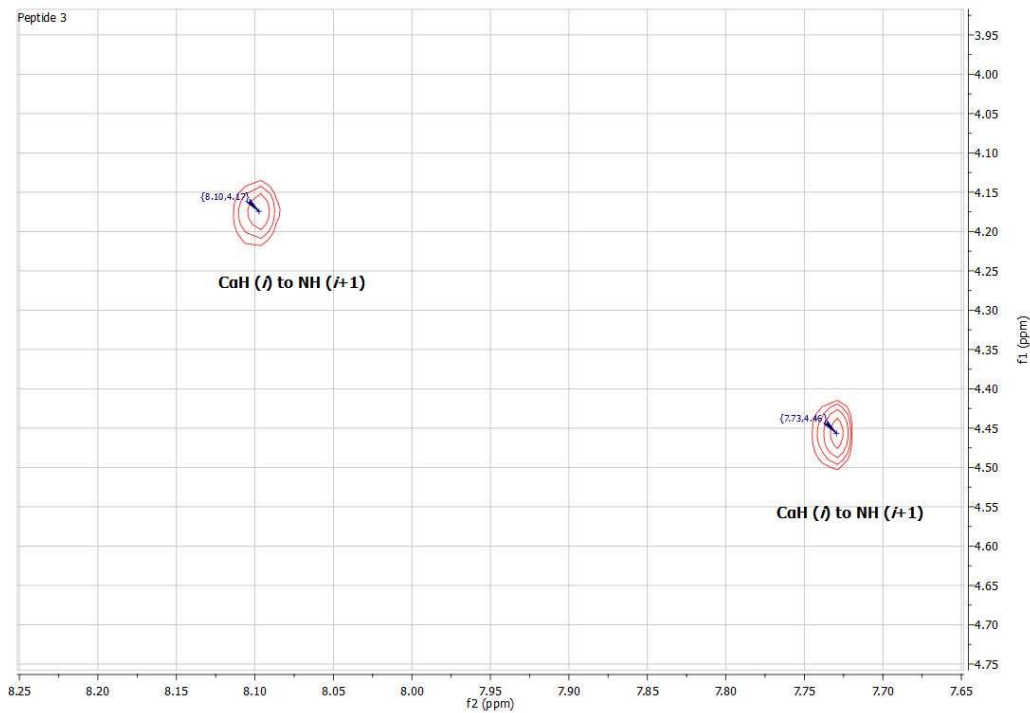


Figure S6. ROESY spectrum of peptide **3** showing CaH (*i*) to NH (*i*+1) interactions.

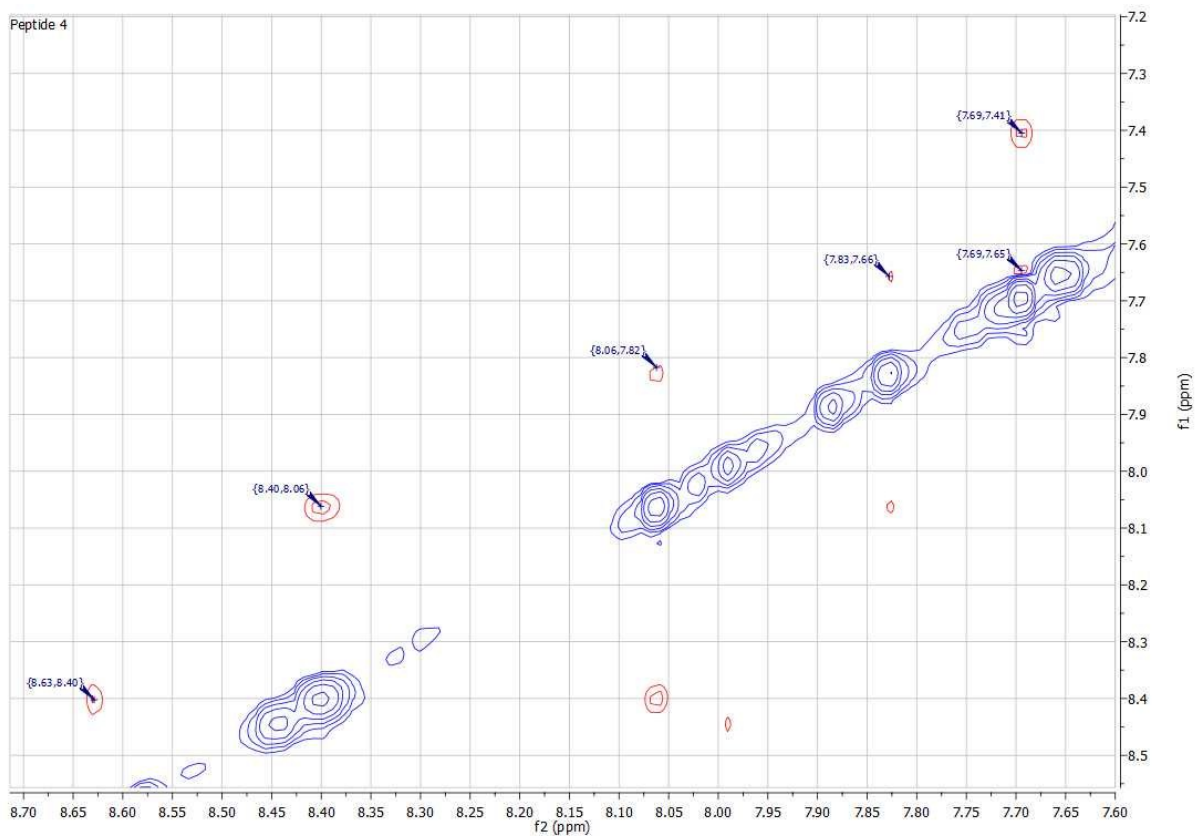


Figure S7. ROESY spectrum of peptide 4 showing NH (*i*) to NH (*i*+1) correlations.



Figure S8. ROESY spectrum of peptide 4 showing CaH (*i*) to NH (*i*+1) interaction.

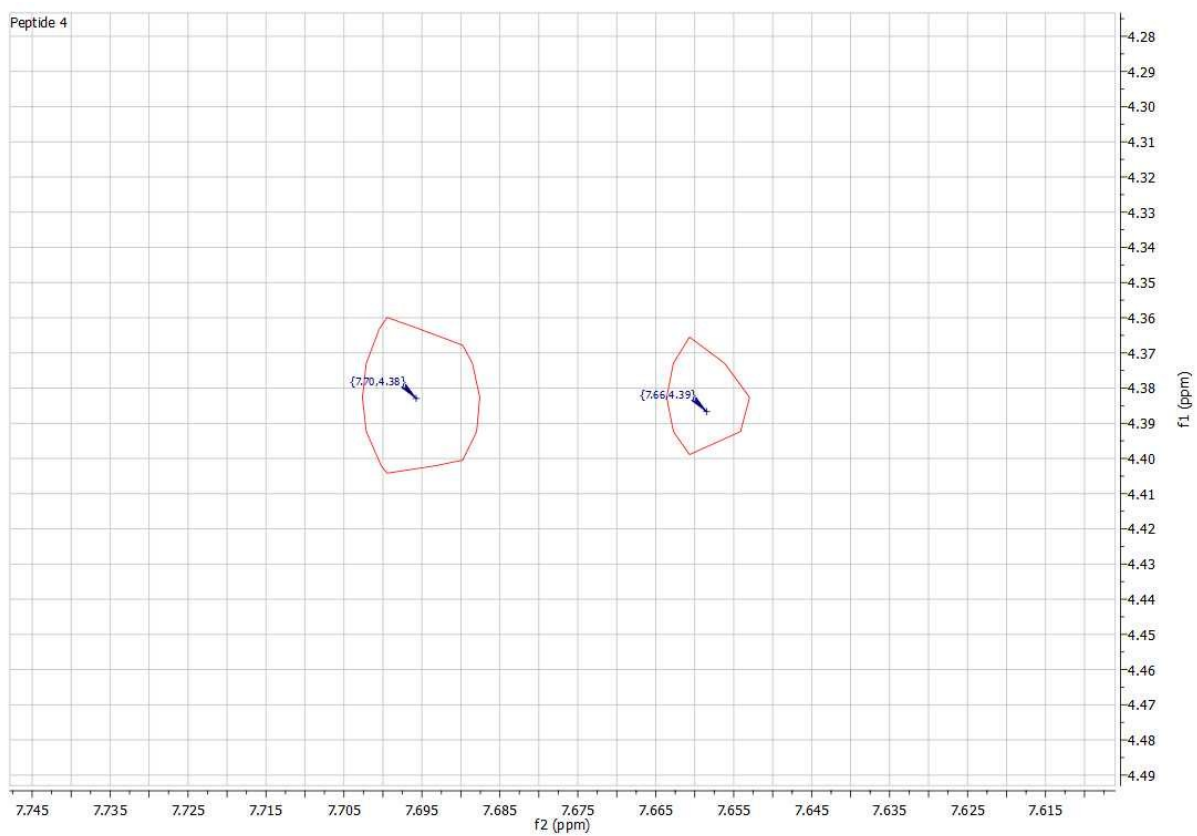


Figure S9. ROESY spectrum of peptide **4** showing the other CaH (*i*) to NH (*i*+1) interaction and to NH (His).

4. ^1H NMR titration study of peptide 3

^1H NMR spectroscopic titration studies were performed to determine the precise peptide/zinc ion complex stoichiometry in peptide 3. The ^1H NMR spectrum for peptide 3 shows a doublet representative of one histidine NH ($\delta = 8.61$ ppm), and another NH ($\delta = 7.56$ ppm) corresponding to the other histidine residue. As Zn^{2+} ions are added to the peptide in solution at 0.2 molar equivalent increments, the signals assigned to both amide hydrogens display upfield shifts of similar magnitude to those observed in the β -strand peptides.

As observed in the β -strand peptide study, these upfield shifts cease when the concentration of zinc ions reaches one molar equivalent. Two and three equivalents of Zn^{2+} ions were added to peptide 3 with no further change to the ^1H NMR spectrum, which supports the formation of a 1:1 peptide/metal complex (see Figure S10). These results also indicate the zinc ion is coordinated to the imidazole moieties of both histidine residues of peptide 3.

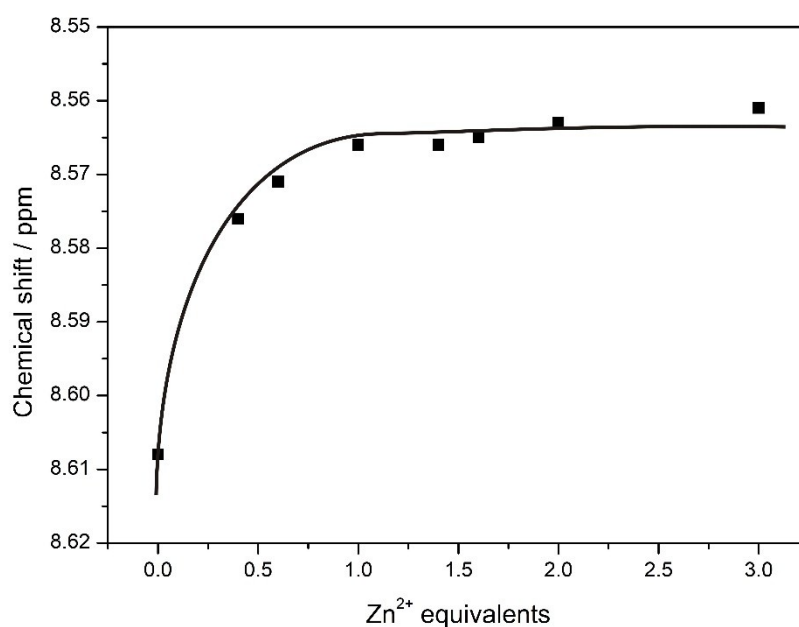


Figure S10. Chemical shifts in the ^1H NMR spectrum for the histidine NH residue of peptide 3 ($\delta = 8.61$ ppm) in the presence of increasing equivalents of Zn^{2+} ions added to the solution. The signal is affected until one equivalent of zinc ions is added. Addition of excess metal ions does not alter the ^1H NMR spectrum, indicating a 1:1 stoichiometry.

5. Computational models of peptides 1 and 3 (unbound and with zinc)

Table S1. Distances critical to the characterization of a β -strand conformation for peptide 1 (unbound and complexed with zinc).

	Ideal antiparallel β -strand distances (\AA) ¹	peptide 1 (\AA)	peptide 1 (with zinc) (\AA)
$\text{C}\alpha\text{H}(i)$ to $\text{NH}(i+1)$	2.2	2.3 - 2.4	2.4 - 2.7
$\text{C}\beta\text{H}_2(i)$ to $\text{NH}(i+1)$	3.2 - 4.5	3.7	3.6
$\text{NH}(i)$ to $\text{NH}(i+1)$	4.3	4.3	2.5 - 4.6
Overall lengths		16.3	14.3

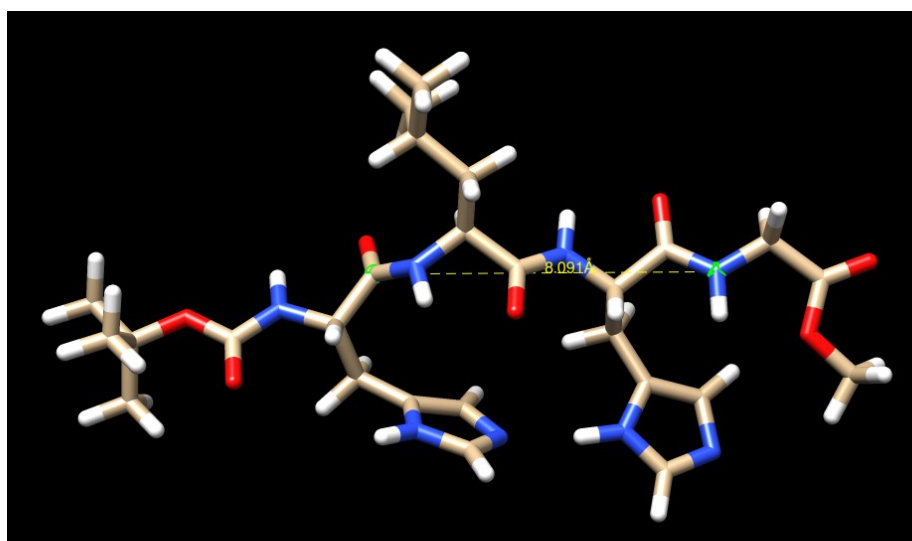


Figure S11. Lowest energy conformer for peptide 1 showing ideal β -strand distance of 8.0 \AA (refer Figure S13).

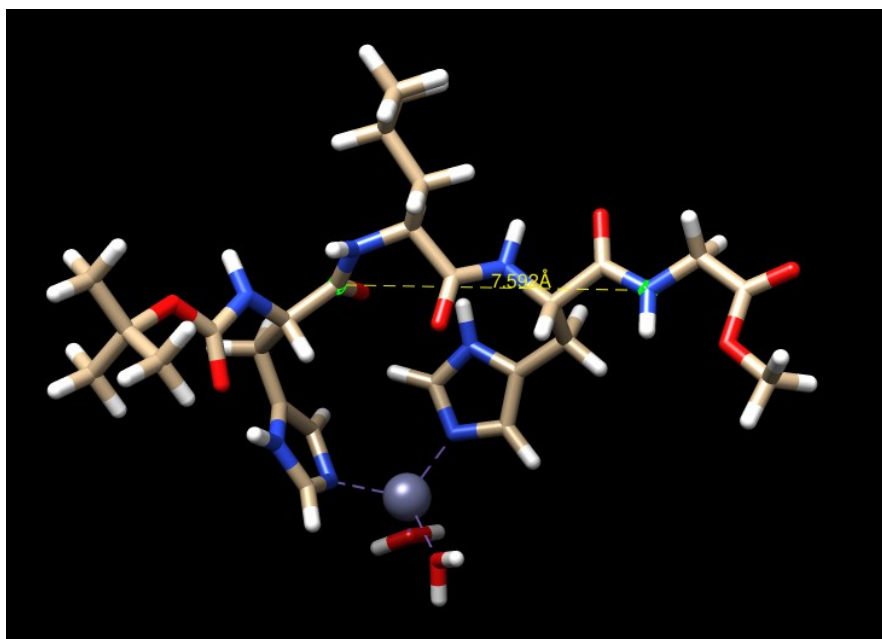


Figure S12. Lowest energy conformer for peptide **1** complexed with zinc, showing 7.5 Å for the same measurement as Figure S11.

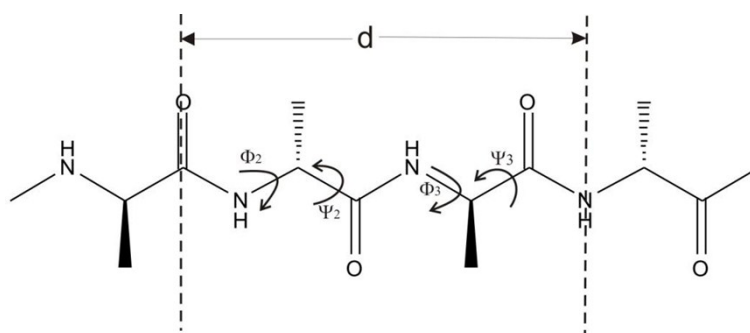


Figure S13. Schematic of ideal peptide β -strand backbone with torsional angles Φ , Ψ , showing optimal distance $d = 8.0 \text{ \AA}$.

Table S2. Backbone dihedral angles for β -strand peptide 1 (unbound and complexed with zinc).

Amino acid residue (ppm)	peptide 1			peptide 1 (with zinc)		
	ϕ	ψ	Ω	ϕ	ψ	Ω
His (7.10)	-161	144	163	-154	30	157
Leu (7.96)	-124	152	-177	-59	155	165
His (8.38)	-144	160	174	-134	162	179
Gly (8.36)	-155	-	-	-	-	-

Table S3. Backbone dihedral angles for peptide 3 (unbound).

- Note. Ideal 3_{10} helical dihedral backbone angles ($\Phi = -57^\circ$, $\psi = -30^\circ$)

peptide 3		
Residue	Φ (degrees)	ψ (degrees)
Aib1	-64	-28
His1	-60	-20
Aib2	-52	-29
Aib3	-58	-17
His2	-88	1
Aib4	-48	-42
AVERAGE	-61	-22
deviates from an ideal 3_{10} -helix by	4	8

Table S4. Backbone dihedral angles for peptide 3 (complexed with zinc).

peptide 3 (complexed with zinc)		
Residue	Φ (degrees)	ψ (degrees)
Aib1	-65	-31
His1	-81	15
Aib2	-59	-37
Aib3	-75	63
His2	-138	29
Aib4	-52	-37

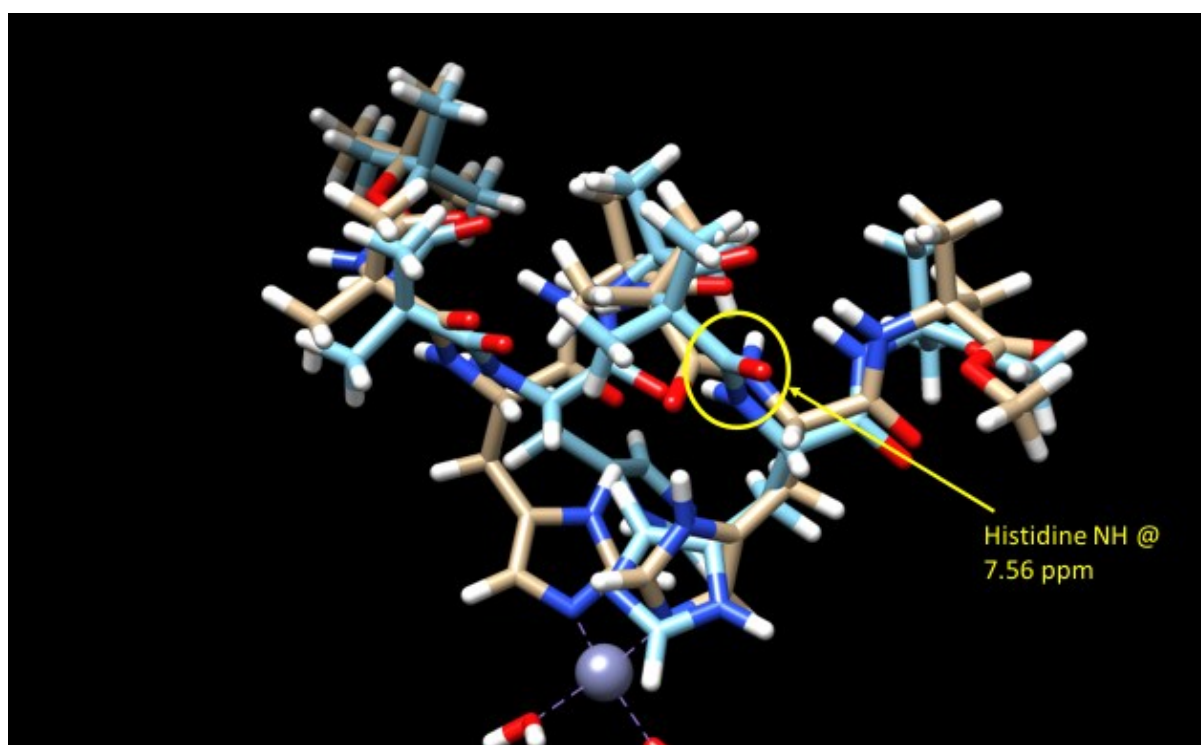


Figure S14. Lowest energy conformers for peptide **3** (unbound and complexed with zinc, overlapped) showing the rotation of the amide hydrogens (blue with white tips) from the second histidine residues (circled).

Table S5. Distances critical to the characterization of a 3_{10} -helical conformation for peptide **3** (unbound and complexed with zinc).

	Ideal 3_{10} -helical distances (Å)	peptide 3 (Å)	peptide 3 (with zinc) (Å)
$C\alpha H (i)$ to $NH (i+1)$	3.4	3.4	3.1
$C\beta H_2 (i)$ to $NH (i+1)$	2.9 – 4.4	3.2 – 4.2	4.0 – 4.5
Overall lengths		13.5	14.7

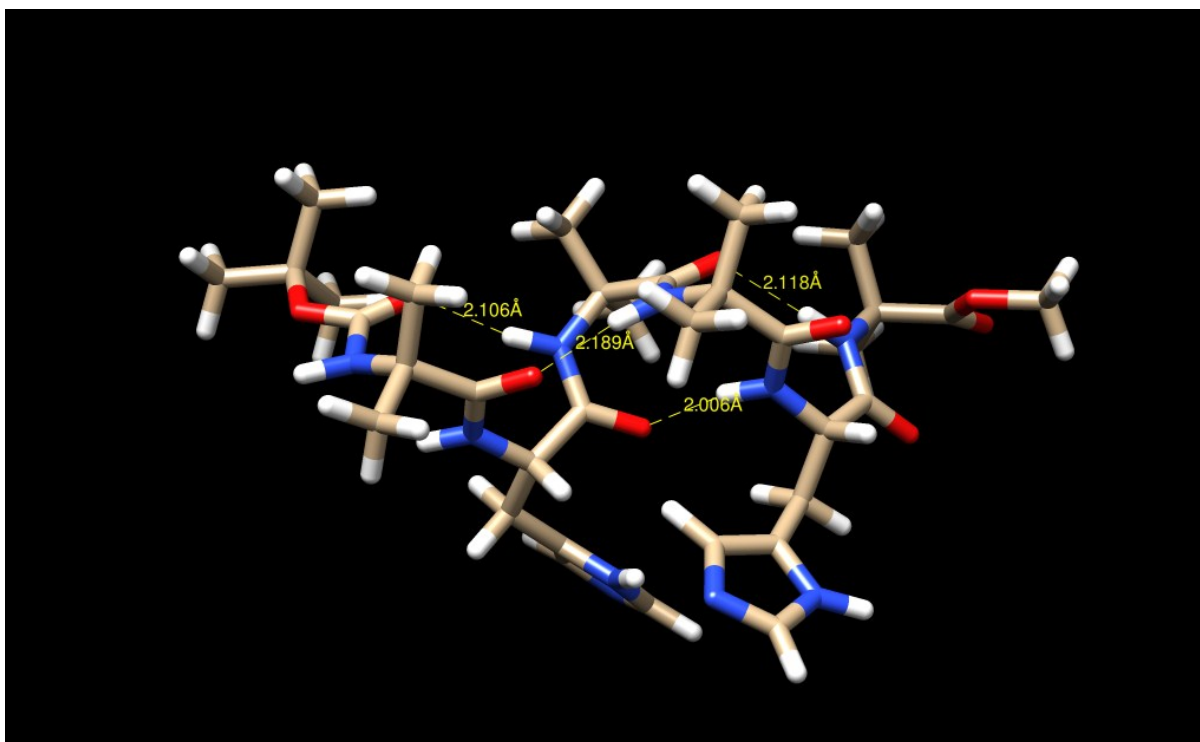


Figure S15. Lowest energy conformer of peptide **3** showing four strong intramolecular hydrogen bonds (i to $i+3$).

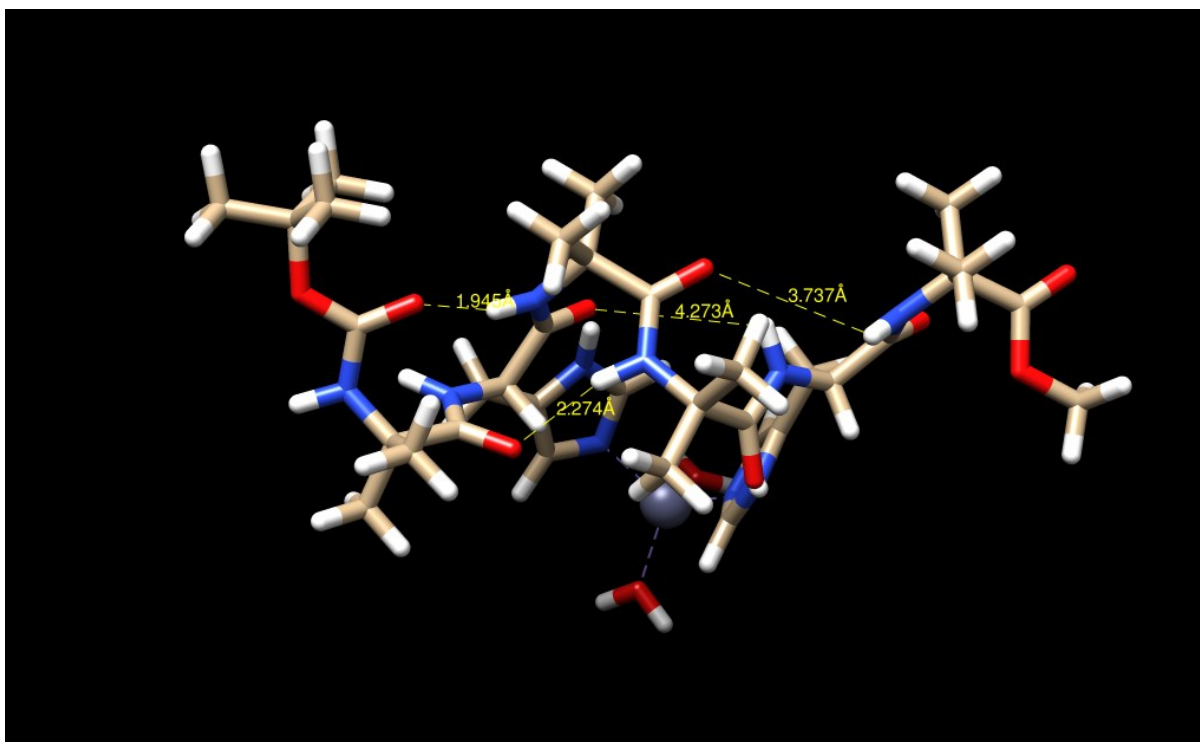


Figure S16. Lowest energy conformer of peptide **3** (complexed with zinc) showing only two strong intramolecular hydrogen bonds (i to $i+3$). The two other possible i to $i+3$ bonds are not suitably orientated, and are classified as weak and outside the permissible range of a 3_{10} -helix.

6. Electrochemical data for peptide 4

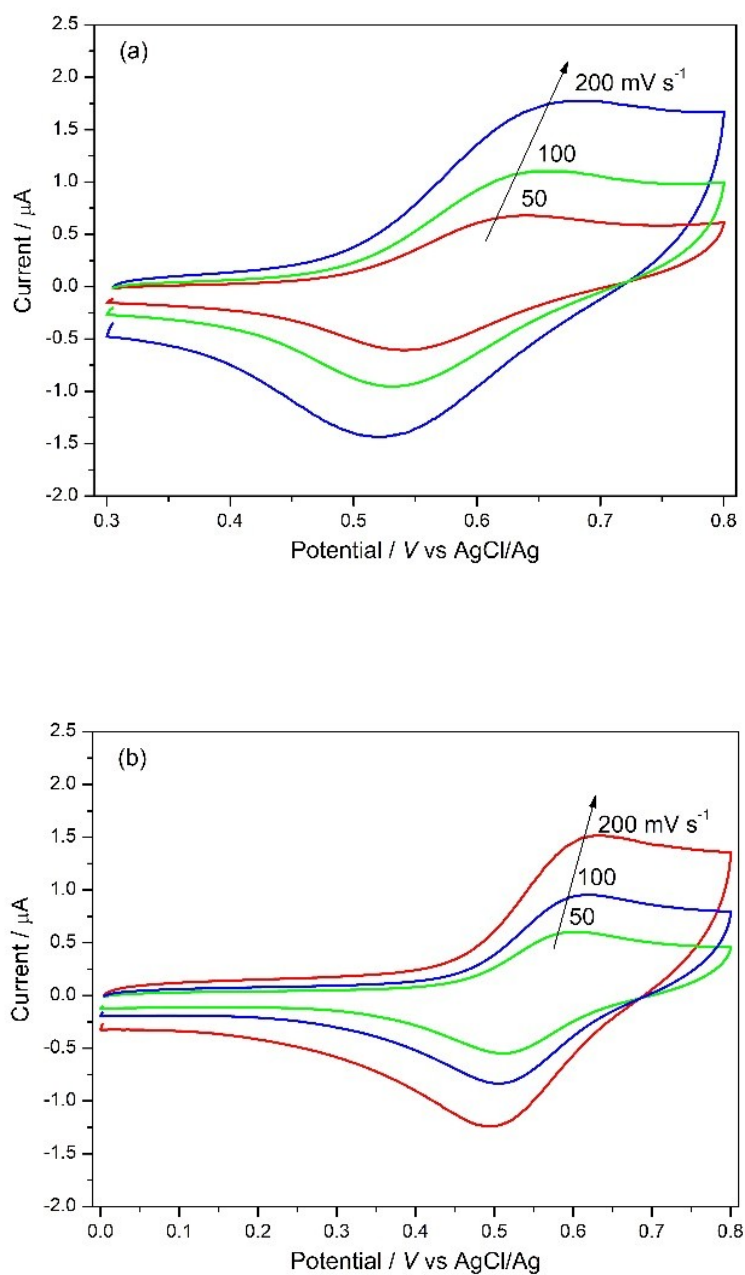


Figure S17. Cyclic voltammograms representative of peptide 4 (a) unbound and (b) complexed with zinc, immobilized onto gold electrodes taken at various scan rates.

7. Switching data for β -strand peptide 2

Here we investigated if the apparent large differential between the electronic properties of the β -strand peptides, with and without zinc, would allow its development as a molecular switch. Hence, a ligand exchange study involving the transfer of zinc ions from the peptide to a chelating agent, ethylenediaminetetraacetic acid (EDTA) was conducted. Specifically, $\text{Zn}(\text{ClO}_4)_2 \cdot 6\text{H}_2\text{O}$ ($1 \mu\text{M}$) and EDTA ($10 \mu\text{M}$) were both separately dissolved in acetonitrile and the switching ability of the peptide was determined by conducting cyclic voltammetry at five minute intervals, alternating between the addition of zinc perchlorate and EDTA to peptide **2**. A total of 18 switching cycles was achieved between peptide **2** (unbound and complexed with zinc, Figure S18) without signal degradation, thus defining the peptide as a robust and reversible electrochemical sensor with potential for metal ion sequestration in biotechnological applications. The reduction in the entropic cost for metal ion binding is a direct result of the pre-organized well-defined secondary structure within the β -strand peptide, thus providing a more efficient zinc ion sensor.

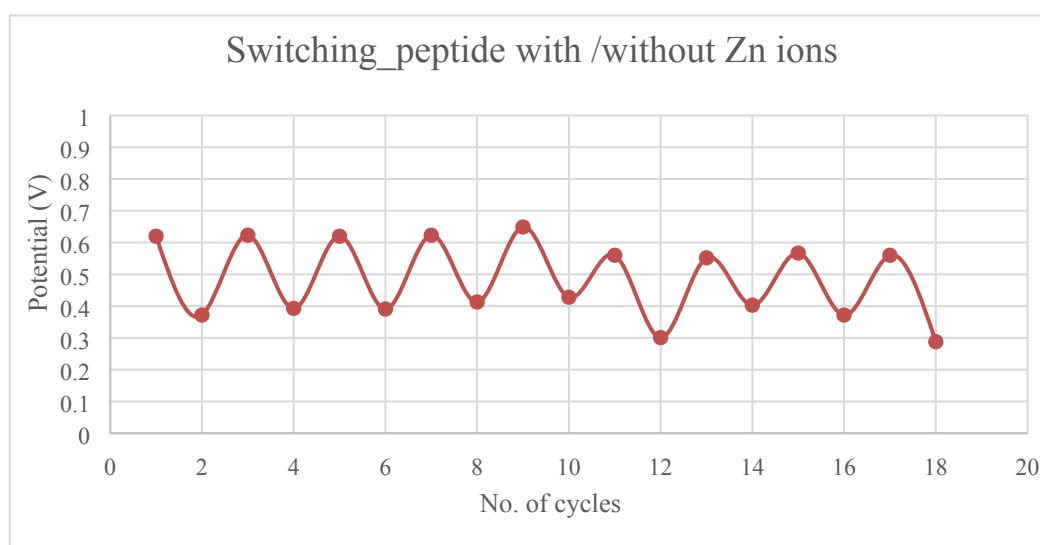


Figure S18. Plot of oxidation peak potential (V) vs number of switching cycles for β -strand peptide **2** (unbound and complexed with zinc).

8. Quantum transport simulations

The molecular junctions were designed using the three system model (extended molecule), including the left electrode lead, central device region, and right electrode lead. The electrode leads were modeled in a $6 \times 6 \times 6$ Au (111) unit cell. Peptide **5** (analogue of **2**, Figure S19) was wired between the gold electrodes via thiol anchoring groups (Figure S20). The structural relaxation of each molecular junction was carried out until the force on each atom was smaller than 0.05 eV/\AA . Subsequent transmission calculations were conducted with the non-equilibrium Green's function approach combined with density functional theory (NEGF-DFT), as implemented in the TranSIESTA computational package.³ This technique yields the transmission spectrum (Figure S21), detailing the probability of an electron with a given energy passing through the junction. Eigenchannels were computed using the Inelastica package.⁴ The valence electronic orbitals of the systems were described using double- ζ polarized basis sets, and a cut-off energy of 250 Ry was used. The Brillouin zone was sampled as a Monkhorst-Pack grid using $4 \times 4 \times 10$ k-points.

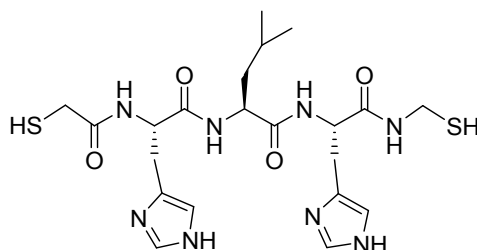


Figure S19. Peptide **5**, analogue of **2**, used for molecular junction simulations.

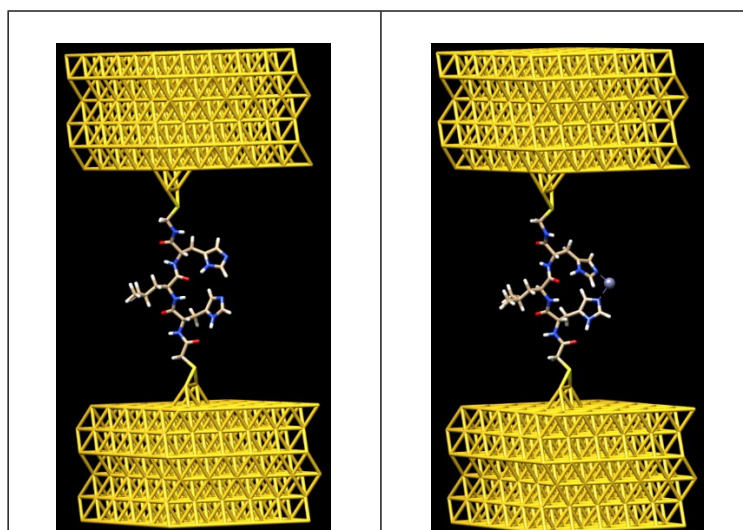


Figure S20. Molecular junctions containing peptide **5** (left) and **5** complexed with zinc (right).

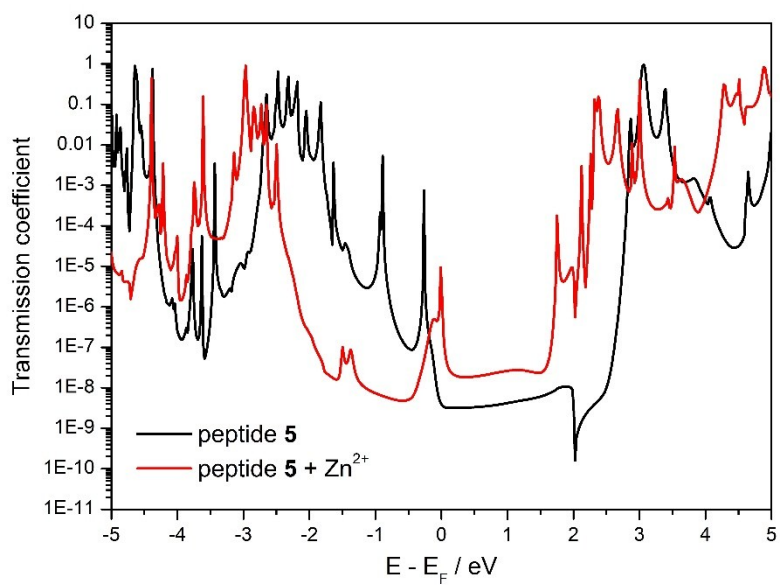


Figure S21. Transmission spectra for peptide **5** (green) and **5** complexed with zinc (red).

9. Constrained density functional theory (cDFT) calculations

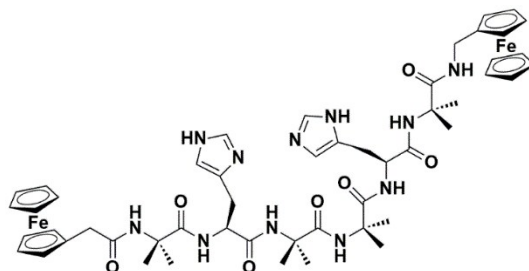


Figure S22. Helical peptide **6**, analogue of **4**, used for donor-acceptor electronic coupling calculations.

Diabatic state calculations were conducted by separately localizing +1 charge on each of the two ferrocene units in **6** using the constrained density functional theory (cDFT). The geometry of each diabatic state was optimized in NWChem 6.6⁵ using the B3LYP density functional, with 6-31G** basis set for all C, H, N, O atoms, and Lanl2dz basis set for Fe atom.

10. Mass Spectroscopy

Sample Name	Zn-008_Gilson_F8	Position	P1-C2	Instrument Name	Instrument 1	User Name	
Inj Vol	3	InjPosition		SampleType	Sample	IRM Calibration Status	Success
Data Filename	Zn-008_Gilson_F8.d	ACQ Method	JHfast-100ACN_3min_r	Comment		Acquired Time	20-Feb-18 10:25:15 AM

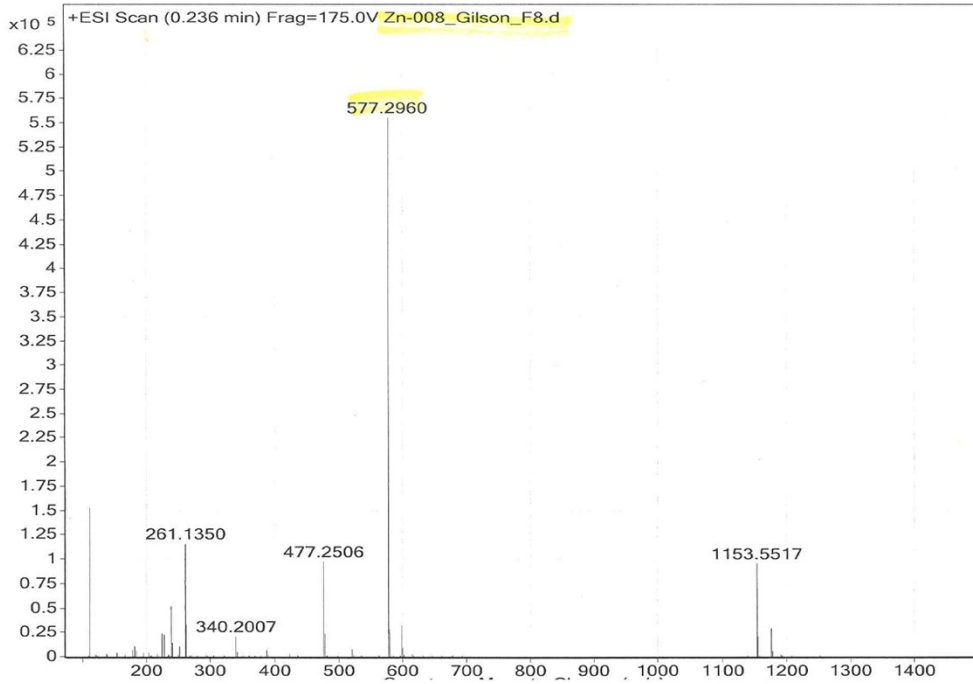


Figure S23. Mass spectrum for peptide 1.

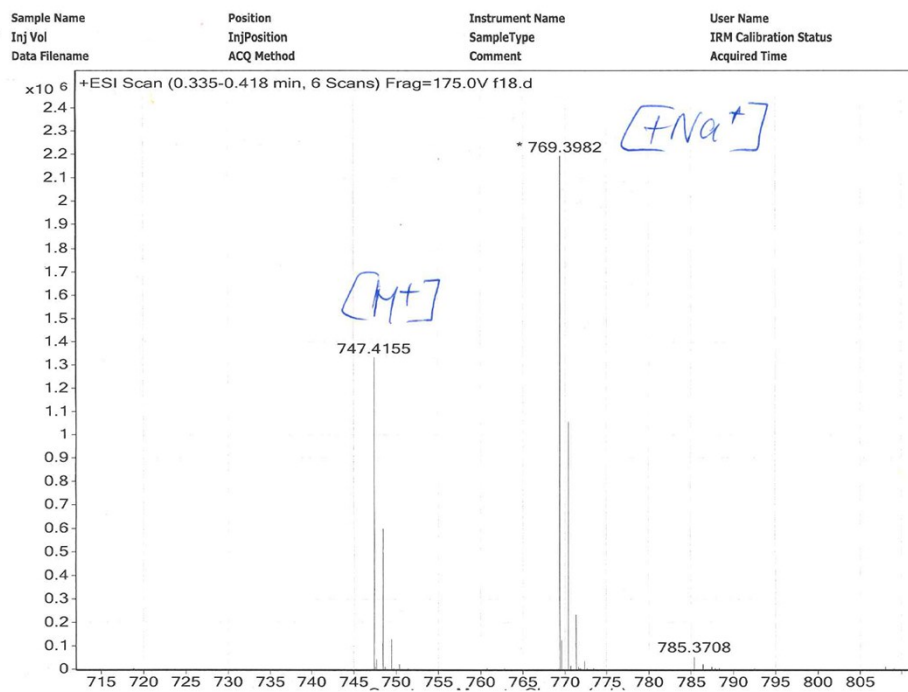


Figure S24. Mass spectrum for peptide 3.

Sample Name	Unavailable	Position	Unavailable	Instrument Name	Unavailable	User Name	Unavailable
Inj Vol	Unavailable	InjPosition	Unavailable	SampleType	Unavailable	IRM Calibration Status	Success
Data Filename	Zn-His-Fc_Gilson F1.	ACQ Method		Comment	Sample information is unavailable	Acquired Time	Unavailable

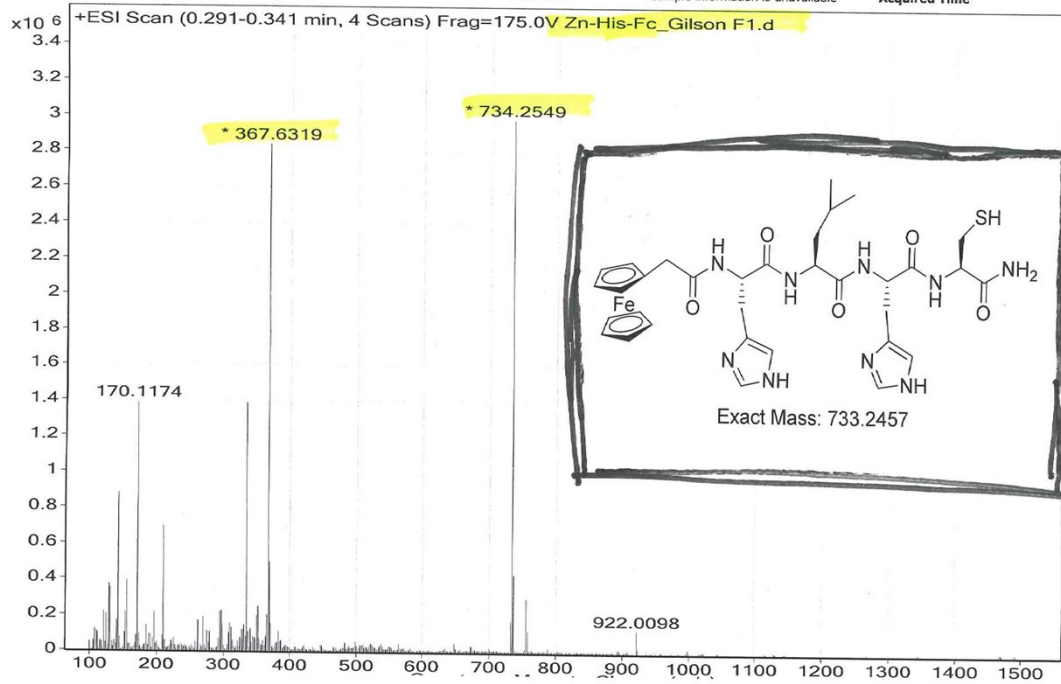


Figure S25. Mass spectrum for peptide 2.

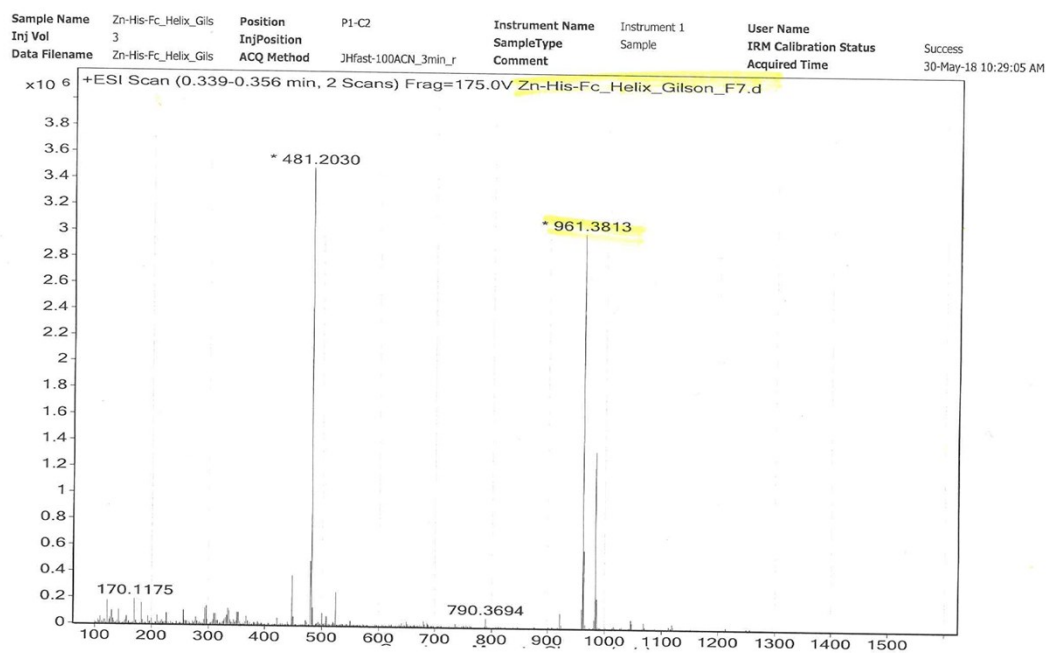
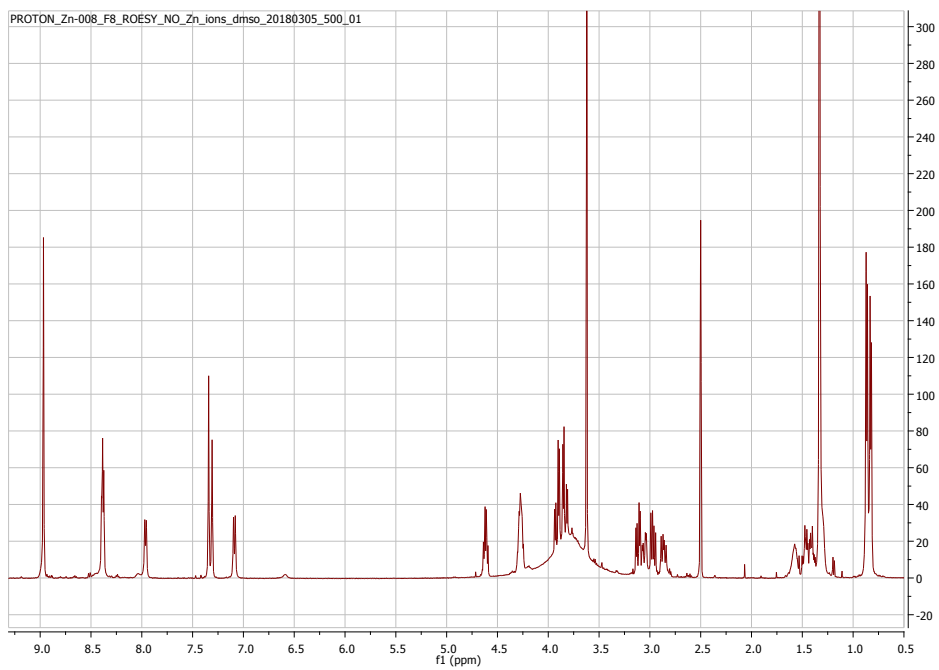


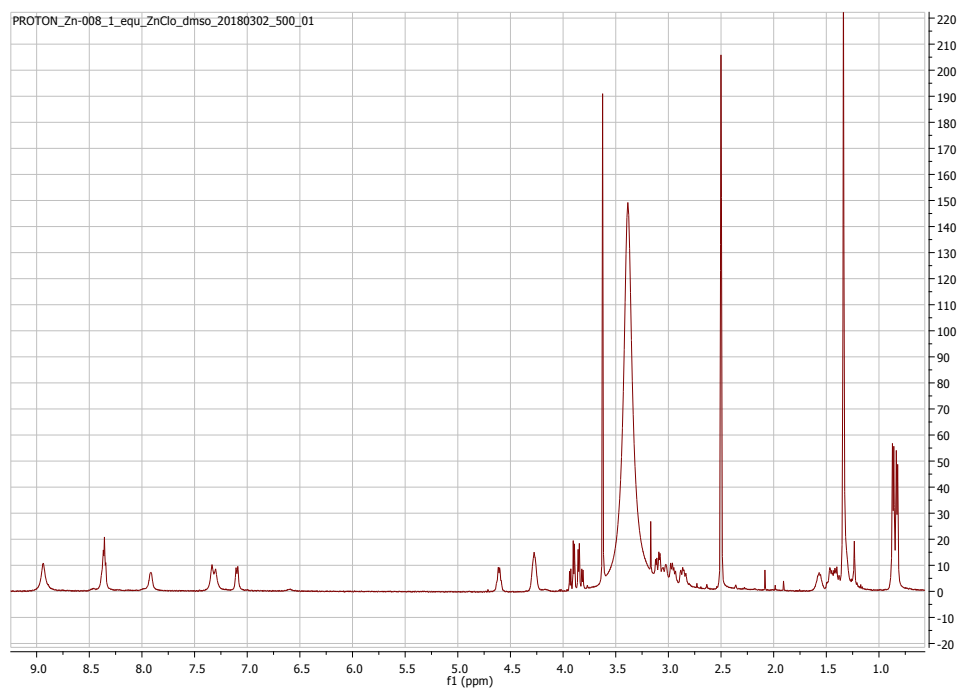
Figure S26. Mass spectrum for peptide 4.

11. ¹H NMR Spectra

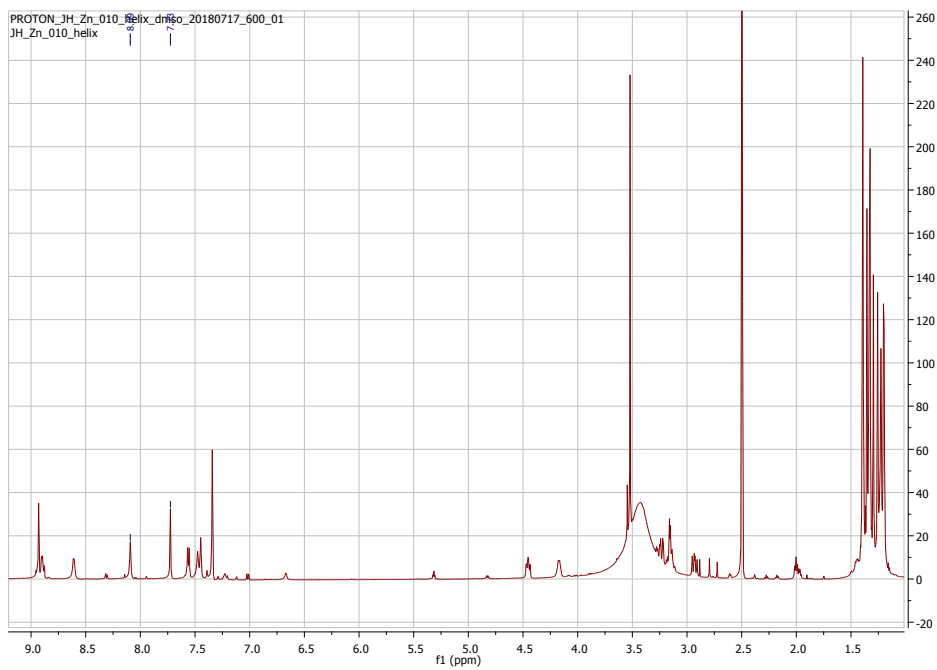
Peptide 1



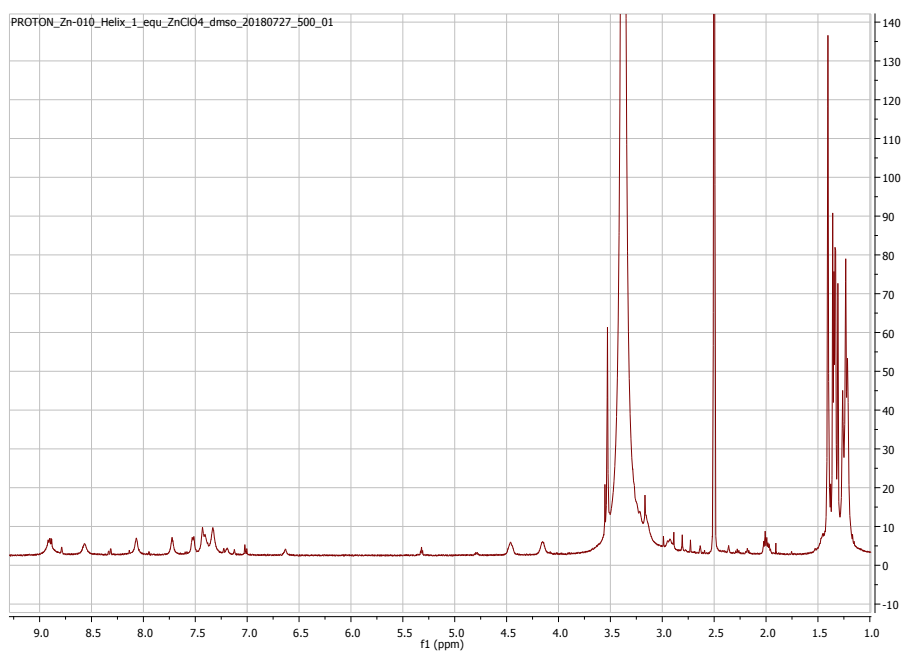
Peptide 1 (complexed with zinc)



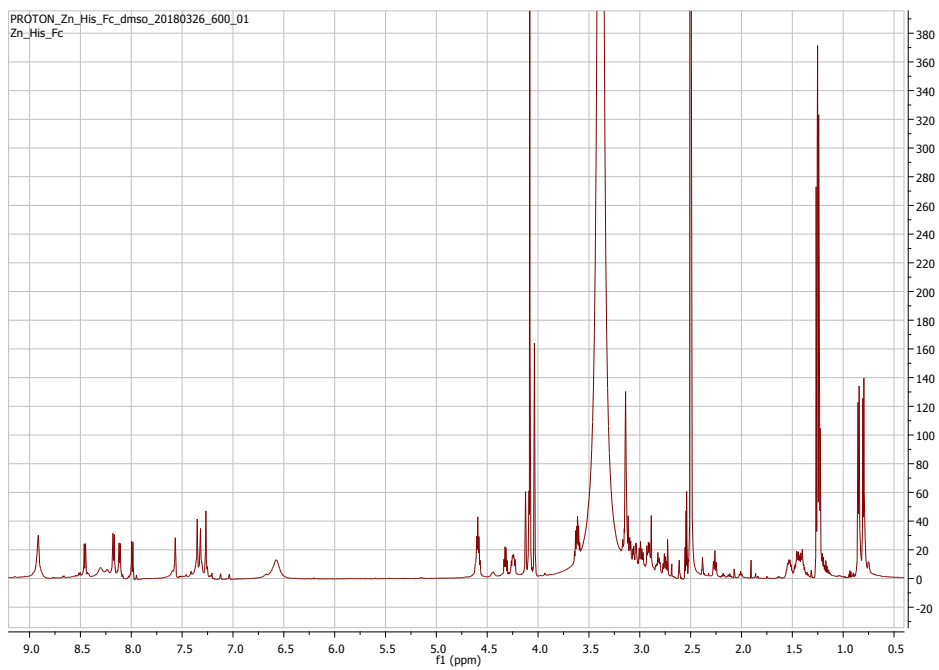
Peptide 3



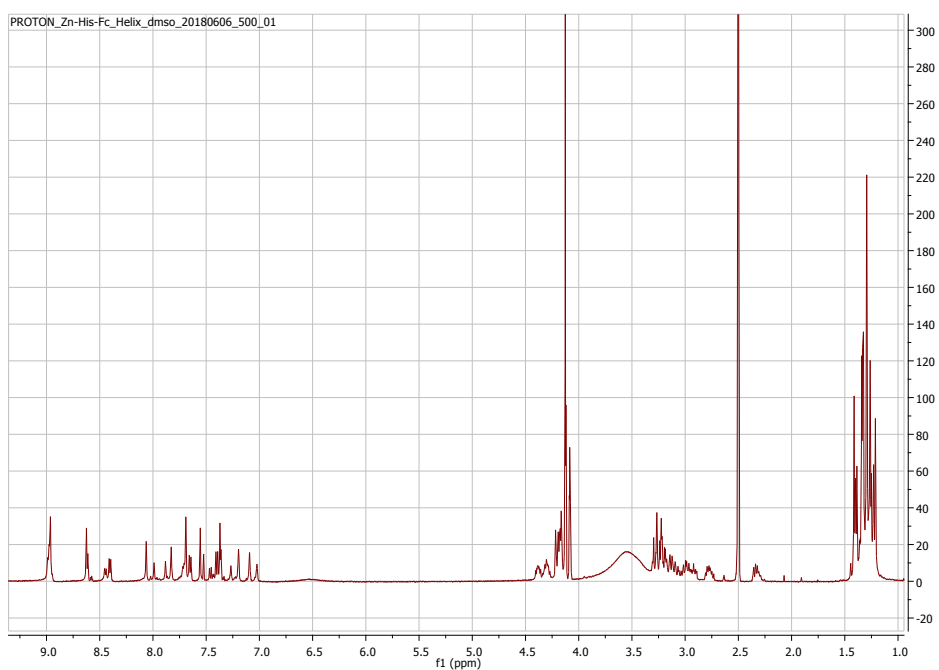
Peptide 3 (complexed with zinc)



Peptide 2



Peptide 4



12. References

1. Wüthrich, K., *NMR of proteins and nucleic acids*. Wiley: 1986.
2. Gillespie, P.; Cicariello, J.; Olson, G. L., *Peptide Science* **1997**, *43*, 191.
3. Brandbyge, M.; Mozos, J. L.; Ordejon, P.; Taylor, J.; Stokbro, K., Density-functional method for nonequilibrium electron transport. *Physical Review B (Condensed Matter and Materials Physics)* **2002**, *65* (16), 165401/1-17.
4. Paulsson, M.; Brandbyge, M., Transmission eigenchannels from nonequilibrium Green's functions. *Physical Review B* **2007**, *76* (11), 15117.
5. Valiev, M.; Bylaska, E. J.; Govind, N.; Kowalski, K.; Straatsma, T. P.; van Dam, H. J. J.; Wang, D.; Nieplocha, J.; Apra, E.; Windus, T. L.; de Jong, W. A., NWChem: a comprehensive and scalable open-source solution for large scale molecular simulations. *Computer Physics Communications* **2010**, *181*, 1477.